Observation of Systematic Variation in Yb Ion Valence as a Function of Interatomic Spacing in Icosahedral Approximant Crystals

Minami Hayashi, Kazuhiko Deguchi, Shuya Matsukawa, Keiichiro Imura, and Noriaki K. Sato*

Department of Physics, Graduate School of Science, Nagoya University, Nagoya 464-8602, Japan

We discovered two alloy systems, Pd-Ga-Yb and Pd-Ge-Yb, that belong to the Tsai-type 1/1 approximant to the Au-Al-Yb quasicrystal exhibiting the unusual quantum criticality and show a similar behavior to Kondo lattice systems with a magnetically ordered ground state. Combining the results of other Yb-based approximant crystals, we find that there is a systematic variation in the Yb ion valence vs the lattice constant. This proves that the Au-Al-Yb approximant is located at the border of the valence change, in favor of the idea that the valence fluctuation plays a crucial role in the quantum criticality of the Au-Al-Yb system.

Quasicrystals (QCs) are metallic alloys that possess long-range, aperiodic structures with diffraction symmetries forbidden to conventional crystals. Recently, the icosahedral QC consisting of Au, Al, and Yb (referred to as the Au-Al-Yb QC hereafter) has attracted much attention as a promising candidate for a critical state unique to QC, which is neither extended nor localized, because a novel quantum criticality was observed in the Au-Al-Yb QC at ambient pressure but not in its approximant crystal (AC),[1)] a crystalline phase that has similar atomic decorations (i.e., Tsai-type icosahedral cluster of atoms) to those of the QC. Here, their magnetic susceptibility χ is expressed as $\chi^{-1} - \chi_0^{-1} \propto T^{\zeta}$ [where $\chi_0 \equiv \chi(T = 0)$ and $\zeta \simeq 0.5$], and the presence/absence of the quantum criticality is confirmed from the absence/presence of the temperature-independent term χ_0.

Interestingly, the quantum criticality survives under pressure for the Au-Al-Yb QC, whereas for the AC, a pressure-induced quantum critical point is observed, as in heavy fermion crystals.[2)] This means that what is important here is not the presence/absence of the quantum criticality at ambient pressure but the difference in the pressure effect on the quantum criticality between the QC and the AC, and strongly suggests that the robust quantum

*E-mail: kensho@cc.nagoya-u.ac.jp

criticality against pressure is related to the critical state unique to the QC.

The question to be addressed now is the origin of the novel quantum criticality of the Au-Al-Yb systems. The same ζ value of the QC and the AC mentioned above suggests the same origin for the QC and the AC. Note that the Yb ion valence in both the QC and the AC fluctuates in time and space between divalence and trivalence.[3,4] Theoretically, the ζ value can be accounted for by the critical valence fluctuation.[5] This suggests that the valence fluctuation plays an important role in the quantum criticality, but no consensus is obtained yet for the origin.[6,7]

Previously, we studied the magnetism of substituted systems (Au-Ga-Yb AC, Ag-Ga-Yb AC, and superconducting Au-Ge-Yb ACs) and found that they are nonmagnetic owing to the divalent Yb ion,[8,9] in contrast to the mixed valence state in the Au-Al-Yb AC. This suggests that a subtle change in the environment of the Yb ion results in the marked change in the Yb ion valence and hence magnetism, which lead us to conjecture that the Au-Al-Yb system is located near the border of divalent and trivalent states of the Yb ion.[8] This conjecture has not yet been proved experimentally. In this study, therefore, we aim at providing experimental evidence supporting this conjecture. Here, we report the discovery of the magnetic systems, the Pd-Ga-Yb AC and the Pd-Ge-Yb AC, that have an Yb ion closer to trivalence than the Au-Al-Yb AC and, as a result, have a magnetically ordered ground state. Studying the magnetism of these and other Yb-based ACs as a function of interatomic spacing, we find that the Au-Al-Yb system is actually located near the border of the valence change. This may be supporting evidence for the scenario that the valence fluctuation plays a crucial role in the unusual quantum criticality.

Before presenting the results, we give a brief description of the geometric structure of the 1/1 AC. According to the structure model of the Au-Al-Yb AC,[10,11] the Tsai-type cluster consists of a concentric arrangement of multiple shells: the first to fifth shells are a Au/Al tetrahedron (that is orientationally disordered), Au/Al dodecahedron, Yb icosahedron, Au/Al icosidodecahedron, and Au/Al triacontahedron, respectively. Here, “Au/Al tetrahedron”, for example, means a tetrahedron in which each atomic site is statistically occupied by Au and Al atoms. Note that the Yb ion site is uniquely positioned at the vertex of the icosahedron. In the AC, the cluster forms a cage network of the body-centered-cubic (bcc) type with the lattice constant of 14.500 Å [see Fig. 1(a)] in which only the outermost triacontahedron is represented for clarity, and the different colors of the small balls distinguish the occupation ratio of the Au and Al atoms (see Ref. 8 for details). Figure 1(b) shows the local environment around the Yb ion; the large centered ball denotes the Yb ion, and the small balls indicate Al

and Au atoms. Note that the (blue) ball at the top indicates the Au/Al atom contained in the outermost triacontahedron, and the two (green) balls at the bottom correspond to the Au/Al atoms of the innermost tetrahedron.[8)]

The purities of starting materials used in the present study were Pd: 99.95, Ga: 99.9999, Ge: 99.999, and Yb: 99.9 wt.%. While these starting materials were arc-melted on a water-cooled copper hearth under argon atmosphere for the Pd-Ga-Yb AC, the starting materials of the Pd-Ge-Yb AC were melted and cooled slowly in an alumina crucible encapsulated by a quartz ampoule under argon atmosphere. No heat treatment was carried out. The alloy composition was nominally $Pd_{30}Ga_{55}Yb_{15}$ and $Pd_{45.6}Ge_{38.9}Yb_{15.5}$, which were determined as $Pd_{29.8}Ga_{56.6}Yb_{13.6}$ and $Pd_{51.3}Ge_{32.8}Yb_{15.9}$, respectively, using the inductively coupled plasma (ICP). The latter composition was used for the following data analysis.

Structure characterization was carried out by means of powder X-ray diffraction using Cu $K\alpha$-radiation. The Rietveld analysis was performed by T. Ishimasa and his group at Hokkaido University. The dc magnetization M was measured using a commercial magnetometer (MPMS, Quantum Design) in the temperature range between 1.8 and 300 K and at magnetic fields H up to 7 T. The ac magnetic susceptibility χ_{ac} was measured by the conventional mutual inductance method, using a commercial dilution refrigerator (μ-Dilution, SAAN) below about 3 K. A modulation field with a frequency of 100.3 Hz and an amplitude of 0.1 Oe was superimposed on a dc magnetic field H supplied by a superconducting magnet. To calibrate the ac magnetic susceptibility, both the dc and ac susceptibilities were measured

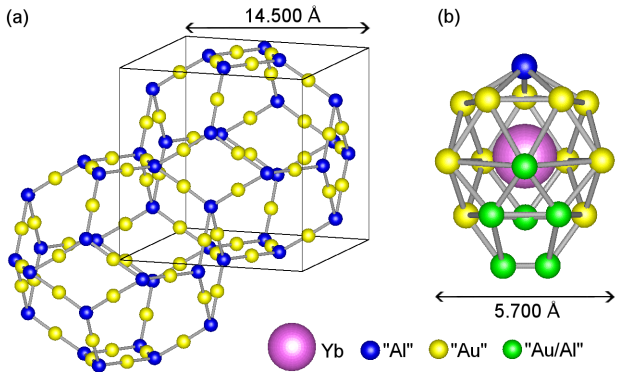

Fig. 1. (Color online) Geometric arrangement of ions in the Au-Al-Yb AC. (a) The bcc-type cage network of the triacontahedron (the outermost shell of the Tsai-type cluster). (b) Local structure around the Yb ion denoted by the large (rose-pink) ball. The small balls in (a) and (b) indicate Au/Al ions: the symbol "Al" indicates the site that is mostly occupied by Al, "Au" denotes the site that is preferably occupied by Au, and "Au/Al" denotes the site that is occupied by Au or Al. The Yb-ion $4f$ state will hybridize with the ligand-ion p state.[8)]

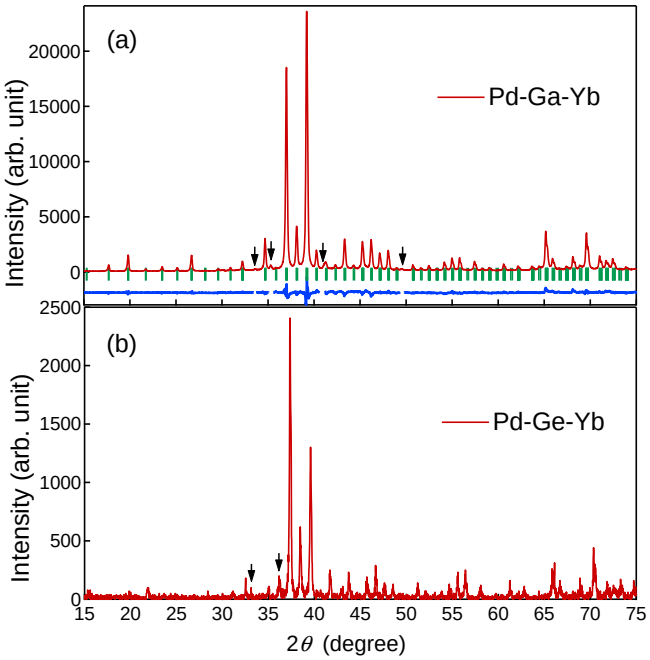

Fig. 2. (Color online) Powder X-ray diffraction patterns of (a) $Pd_{29.8}Ga_{56.6}Yb_{13.6}$ and (b) $Pd_{51.3}Ge_{32.8}Yb_{15.9}$. The nominal compositions of these samples were $Pd_{30}Ga_{55}Yb_{15}$ and $Pd_{45.6}Ge_{38.9}Yb_{15.5}$, respectively. The arrows mark the secondary phases.

in the same temperature interval at each dc magnetic field. The specific heat was measured by the quasi-adiabatic method, using a commercial ^{3}He cryostat (Heliox, Oxford Instruments).

Figure 2(a) shows a powder X-ray diffraction pattern of $Pd_{29.8}Ga_{56.6}Yb_{13.6}$. Bragg reflections are indicated by the short (green) bars below the pattern. The difference between calculation and measurement is indicated by the lowermost (blue) curves. Several weak lines denoted by arrows are ascribed to a secondary phase, possibly the YbPdGa phase. Removing these lines, we analyzed the diffraction pattern to determine the lattice parameter and the atomic coordinates by the Cohen's and Rietveld method, and we confirmed that the obtained sample belongs to the Tsai-type 1/1 AC with the lattice parameter of 14.15 Å. Figure 2(b) shows a powder X-ray diffraction pattern of $Pd_{51.3}Ge_{32.8}Yb_{15.9}$. Secondary phases are marked by the arrows. The Rietveld analysis was not carried out and only the lattice parameter was estimated as $a = 14.01$ Å. Although the atomic coordination was not determined, the main phase of the sample was confirmed to be the Tsai-type 1/1 AC. At present, the secondary phases in the two ACs synthesized here are not identified. In this study, we assume that these phases do not seriously affect the present results.

Figure 3 shows the temperature dependences of the inverse dc susceptibility H/M. We observe that both the Pd-Ga-Yb AC and the Pd-Ge-Yb AC show the Curie–Weiss-like straight-

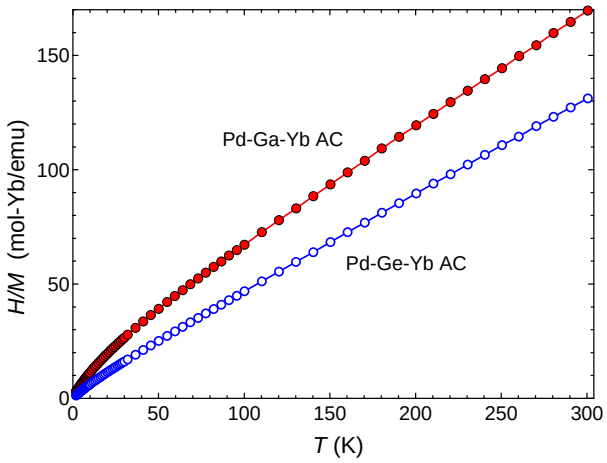

Fig. 3. (Color online) Temperature dependence of H/M of the Pd-Ga-Yb AC (red filled circles) and the Pd-Ge-Yb AC (blue open circles) measured at $H = 1$ kOe. The lines between the data points are guides for the eye.

line feature above about 100 K with a convex curvature below about 50 K. The linear slope of the curves above ~100 K yields effective magnetic moments of $p_{\rm eff} = 3.96$ and 4.35 $\mu_{\rm B}$/Yb for the Pd-Ga-Yb AC and the Pd-Ge-Yb AC, respectively. Upon comparing these $p_{\rm eff}$ values with the free Yb^{3+} ion value (4.54 $\mu_{\rm B}$), we suggest that the electrons are almost localized at high temperatures for both the ACs, and further that the mixed-valence nature is stronger in the Pd-Ga-Yb AC than in the Pd-Ge-Yb AC. To directly confirm the valence states of these materials, we need to carry out further experiments such as photoemission spectroscopy.

We measured the dc magnetization M at low temperatures (not shown here), and observed that M initially increases linearly with the magnetic field H and tends to saturate above $H \sim 30$ kOe; at 70 kOe, $M \simeq 1.0$ and 1.8 $\mu_{\rm B}$/Yb for the Pd-Ga-Yb AC and the Pd-Ge-Yb AC, respectively. Note that the low-temperature saturated moment is substantially reduced compared with the free-ion-like moment observed at high temperatures. As similar behavior was observed in the non-Kondo system, Au-Al-Tm AC,[12] this moment reduction is primarily ascribed to the crystal field effect in these systems.

Figure 4(a) shows the ac susceptibility $\chi_{\rm ac}$ and the dc susceptibility $\chi_{\rm dc} \equiv M/H$ of the Pd-Ga-Yb AC (upper panel) and the Pd-Ge-Yb AC (lower panel). The dc fields H applied here are denoted in the lower panel. At $H = 0$, both the ACs show a round peak at $T_{\rm f} \simeq 0.2$ K. This peak structure is suppressed by the application of external field; a field less than 1 kOe is sufficient to completely depress the peak. This magnetic field effect on the $\chi_{\rm ac}(T)$ curves is reminiscent of the spin-glass system, suggesting the possibility of the peak being

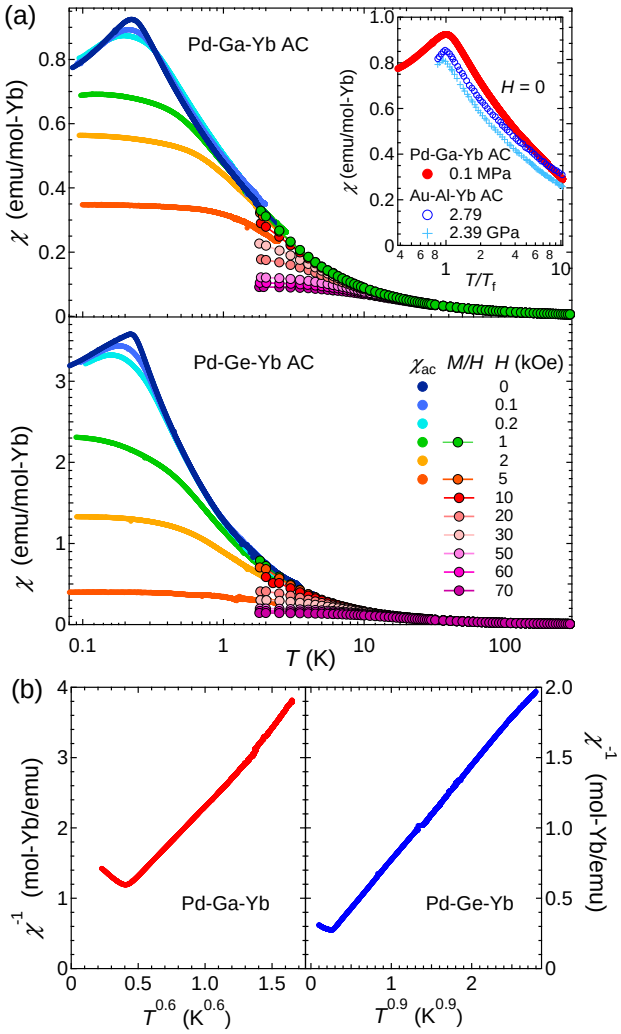

Fig. 4. (Color online) (a) Temperature dependence of the magnetic susceptibilities of the Pd-Ga-Yb AC (upper panel) and the Pd-Ge-Yb AC (lower panel). The ac and dc susceptibilities were measured at $T \lesssim 3$ K and $T \gtrsim 1.8$ K, respectively. H denotes the dc field measured. The inset shows the temperature dependence of the ac susceptibility of the ambient-pressure (0.1 MPa) Pd-Ga-Yb AC and the high-pressure Au-Al-Yb AC. (b) Inverse magnetic susceptibilities of the Pd-Ga-Yb AC (left panel) and the Pd-Ge-Yb AC (right panel) as functions of $T^{0.6}$ and $T^{0.9}$, respectively. The straight line feature is observed for the Pd-Ga-Yb AC and the Pd-Ge-Yb AC in the temperature range between 0.26 and 1.7 K and between 0.21 and 2.6 K, respectively.

due to a spin-glass-like transition. At $H \gtrsim 1$ kOe, the ac susceptibility curves show a heavy-fermion-like feature; as the temperature decreases, the susceptibility monotonically increases and tends to saturate at a high susceptibility, which, by analogy with heavy fermions, arises from the high density of states at the Fermi energy. This allows us to regard the present systems as Kondo systems, which can be characterized by the Kondo temperature $T_{\rm K}$. Since the Pauli susceptibility is inversely proportional to $T_{\rm K}$, the Pd-Ga-Yb AC is considered to

have a higher T_K than the Pd-Ge-Yb AC.

In the inset of Fig. 4(a), the Pd-Ga-Yb AC is compared with the high-pressure phase of the Au-Al-Yb AC in which the spin-glass-like transition was confirmed to occur below $T_f \simeq 0.1$ K from the frequency dependence of the peak temperature.[13] Interestingly, the Pd-Ga-Yb AC shows a similar feature to the pressurized Au-Al-Yb AC for $T/T_f \gtrsim 1$. This similarity has twofold implications. Firstly, it may strengthen the possibility of the spin-glass-like transition in the Pd-Ga-Yb AC. Secondly, it leads us to expect that the Pd-Ga-Yb AC has a similar exponent ζ of the susceptibility to that of the Au-Al-Yb AC (i.e., $\zeta \simeq 0.5$). This is confirmed by plotting the data in the form of χ^{-1} vs T^{ζ} [see the left panel of Fig. 4(b)], in which we observe the straight line feature for $\zeta \simeq 0.6$.

The right panel of Fig. 4(b) shows $\zeta \simeq 0.9$ for the Pd-Ge-Yb AC. Note that this ζ value is close to $\zeta = 1$ corresponding to the conventional Curie–Weiss law as observed in the Au-Al-Tm AC, a typical localized moment system.[12] On the basis of the combined results for the Pd-Ga-Yb AC, the Pd-Ge-Yb AC, and the Au-Al-Tm AC, we suggest the possibility of a correlation between ζ and T_K such that ζ approaches 1 as $T_K \to 0$. Here, we assumed that the localized moment system such as the Au-Al-Tm AC is regarded as a system with $T_K = 0$.

Figure 5 shows the temperature dependence of the heat capacity divided by temperature, C/T. We find that it exhibits the heavy-fermion feature, consistent with the result suggested from the susceptibility measurement. Unfortunately, however, we could not confirm if it is consistent with our above interpretation of the spin-glass-like transition, in other words, if a sharp anomaly is absent near T_f, because the base temperature of the measurement, ~ 0.35

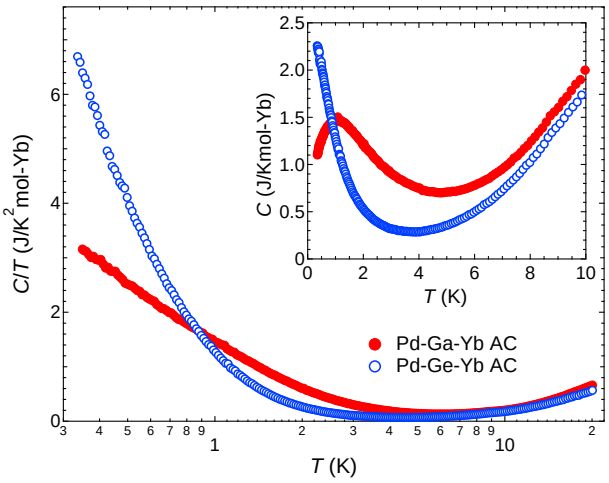

Fig. 5. (Color online) Temperature dependence of the specific heat divided by temperature, C/T, of the Pd-Ga-Yb AC and the Pd-Ge-Yb AC. The inset shows the temperature dependence of C.

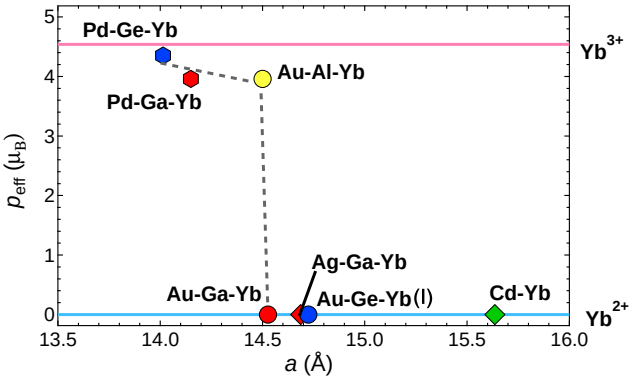

Fig. 6. (Color online) Plot of the effective Bohr magneton $p_{\rm eff}$ vs the lattice parameter a. The broken line is a guide for the eye.

K, was above $T_{\rm f}$.

Let us make two brief comments on the temperature dependence of the specific heat. First, we observe that C/T exhibits the logarithmic temperature dependence in a temperature interval above $T_{\rm f}$. Whether this is a critical phenomenon should be confirmed in the future. Second, we observe that the specific heat C of the Pd-Ga-Yb AC shows a broad peak at about 1 K; see the inset of Fig. 5. Its origin is yet unclear, but some possibilities are proposed: the crystal field effect, the onset of the spin-glass-like transition, and the Kondo peak. This should also be clarified in the future.

Figure 6 summarizes the relationship of the lattice parameter a with the effective moment $p_{\rm eff}$ deduced from the high-temperature susceptibility, together with published data.[8,9,14] It is interesting to note that a sharp change occurs at $a_{\rm c} \sim 14.5$ Å. This critical lattice parameter $a_{\rm c}$ separates the materials into two groups: the magnetic group with $a \lesssim a_{\rm c}$ (Pd-Ge-Yb, Pd-Ga-Yb, and Au-Al-Yb) and the nonmagnetic group with $a \gtrsim a_{\rm c}$ (Au-Ga-Yb, Ag-Ga-Yb, and Au-Ge-Yb). We stress that the Au-Al-Yb AC is located near $a_{\rm c}$, which is one of the primary results of the present study. This is compatible with the fact that the smaller lattice constant favors the magnetic Yb^{3+} state,[8] and also with the pressure effect mentioned above. When applying external pressure on the Au-Al-Yb AC, the magnetic ordered state emerges, as observed in the ambient-pressure Pd-Ga-Yb AC.[2,13]

The substitution effect is numerically summarized in Table I. We find that the substitution Au $\leftrightarrow$ Pd gives rise to a larger change in the lattice parameter than does Al $\leftrightarrow$ Ga $\leftrightarrow$ Ge. (Note that, for example, the substitution Au $\rightarrow$ Pd does not mean a one-to-one replacement of Pd for Au, as may be seen from the comparison of the composition between $Au_{44}Ga_{41}Yb_{15}$ and $Pd_{29.8}Ga_{56.6}Yb_{13.6}$; the Au sites are occupied by not only Pd but also Ga.) This indicates that

Table I. Summary of the substitution effect. The composition of ACs other than the Pd-Ga-Yb AC and the Pd-Ge-Yb AC is nominal. Δa indicates the lattice-constant change upon substitution, and the positive and negative values denote lattice expansion and shrinkage, respectively.

Symbolic notation	Approximant crystal with composition	Δa
Au → Pd	$Au_{44}Ga_{41}Yb_{15} \rightarrow Pd_{29.8}Ga_{56.6}Yb_{13.6}$	-0.38Å
Au → Pd	$Au_{64}Ge_{22}Yb_{14} \rightarrow Pd_{51.3}Ge_{32.8}Yb_{15.9}$	-0.71Å
Al → Ga	$Au_{49}Al_{36}Yb_{15} \rightarrow Au_{44}Ga_{41}Yb_{15}$	+0.03Å
Al → Ge	$Au_{49}Al_{36}Yb_{15} \rightarrow Au_{64}Ge_{22}Yb_{14}$	+0.22Å
Ga → Ge	$Au_{44}Ga_{41}Yb_{15} \rightarrow Au_{64}Ge_{22}Yb_{14}$	+0.20Å
Ga → Ge	$Pd_{29.8}Ga_{56.6}Yb_{13.6} \rightarrow Pd_{51.3}Ge_{32.8}Yb_{15.9}$	-0.14Å

the transition metal ion (Pd and Au), which constitutes the outermost shell (triacontahedron) forming the bcc structure [see Fig. 1(a)], plays a primarily role in the determination of the Yb valence via the lattice parameter.

Note that the Au-Al-Yb AC and the Au-Ga-Yb AC have the similar lattice constants but different valences. This can be understood by assuming that the Al $3p$ states and the Ga $4p$ states contribute to the conduction band formation,[15] and the former is more hybridized with the Yb $4f$ states than the latter. This means that the p-electron element (Al, Ga, and Ge) also plays an important role in the determination of the Yb valence via the mixing effect with the ligand [see Fig. 1(b)].

To summarize, we found two new alloy systems, Pd-Ga-Yb and Pd-Ge-Yb, that belong to the group of 1/1 ACs with the Tsai-type cluster and show magnetic susceptibility and specific heat similar to those of Kondo systems. At the low temperature $T_f \simeq 0.2$ K, they show a peak structure in the ac magnetic susceptibility, possibly owing to the emergence of the spin-glass-like short-range ordered state. The discovery of these new materials enabled us to reveal that there is a sharp change in the Yb ion valence as a function of the lattice constant, indicating that the Au-Al-Yb AC is located at the border of the valence change. We discussed the possibility that there is a correlation between the critical exponent ζ of the susceptibility and the Kondo temperature T_K such that ζ approaches 1 as $T_K \rightarrow 0$.

Acknowledgment

The authors thank T. Ishimasa for carrying out the Rietveld analysis and for critical reading of the manuscript. This work was financially supported by a Grant-in-Aid for Scientific Research from JSPS, KAKENHI (Nos. 26610100, 15H02111, 15H03685, and 16H01071), and Program for Leading Graduate Schools “Integrative Graduate Education and Research

Program in Green Natural Sciences", MEXT, Japan.

References

1) K. Deguchi, S. Matsukawa, N. K. Sato, T. Hattori, K. Ishida, H. Takakura, and T. Ishimasa, Nat. Mater. **11**, 1013 (2012).

2) S. Matsukawa, K. Deguchi, K. Imura, T. Ishimasa, and N. K. Sato, J. Phys. Soc. Jpn. **85**, 063706 (2016).

3) T. Watanuki, S. Kashimoto, D. Kawana, T. Yamazaki, A. Machida, Y. Tanaka, and T. J. Sato, Phys. Rev. B **86**, 094201 (2012).

4) M. Matsunami, private communication.

5) S. Watanabe and K. Miyake, J. Phys. Soc. Jpn. **82**, 083704 (2013).

6) V. R. Shaginyan, A. Z. Msezane, K. G. Popov, G. S. Japaridze, and V. A. Khodel, Phys. Rev. B **87**, 245122 (2013).

7) E. C. Andrade, A. Jagannathan, E. Miranda, M. Vojta, and V. Dobrosavljevic, Phys. Rev. Lett. **115**, 036403 (2015).

8) S. Matsukawa, K. Tanaka, M. Nakayama, K. Deguchi, K. Imura, H. Takakura, S. Kashimoto, T. Ishimasa, and N. K. Sato, J. Phys. Soc. Jpn. **83**, 034705 (2014).

9) K. Deguchi, M. Nakayama, S. Matsukawa, K. Imura, K. Tanaka, T. Ishimasa, and N. K. Sato, J. Phys. Soc. Jpn. **84**, 023705 (2015).

10) A. P. Tsai, J. Q. Guo, E. Abe, H. Takakura, and T. J. Sato, Nature **408**, 537 (2000).

11) T. Ishimasa, Y. Tanaka, and S. Kashimoto, Philos. Mag. **91**, 4218 (2011).

12) M. Nakayama, K. Tanaka, S. Matsukawa, K. Deguchi, K. Imura, N. K. Sato, H. Takakura, and T. Ishimasa, J. Phys. Soc. Jpn. **84**, 024721 (2015).

13) S. Matsukawa, K. Deguchi, K. Imura, T. Ishimasa, and N. K. Sato, Proceedings of the International Conference on Quasicrystals, 2016.

14) S. K. Dhar, A. Palenzona, P. Manfrinetti, and S. M. Pattalwar, J. Phys.: Condens. Matter **14**, 517 (2002).

15) S. Watanabe and K. Miyake, J. Phys. Soc. Jpn. **85**, 063703 (2016).